THE JOURNAL OF PHYSICAL CHEMISTRY B

 VOLUME 107, NUMBER 8, FEBRUARY 27, 2003

LETTERS

Direct Structural and Chemical Analysis of Individual Core−Shell (Pd, Sn) Nanocolloids

Olaf Holderer,[†,‡] Thierry Epicier,*[,†] Claude Esnouf,[†] and Gilbert Fuchs[‡]

GEMPPM, umr CNRS 5510, INSA de Lyon, 69621 Villeurbanne Cedex, France, and ATOFINA−Centre de Recherche Rhône-Alpes, BP 22, 69493 Pierre-Benite Cedex, France

Received: April 25, 2002; In Final Form: October 22, 2002

Palladium−tin nanocolloids have been analyzed with high-resolution transmission electron microscopy (HRTEM) and electron energy-loss spectroscopy (EELS). The composition of individual colloids with a diameter of 2−5 nm has been deduced. It has been established that the colloids consist of a core of a Pd_xSn_{1-x} alloy, with x ranging from 0.6 to 1. From the numerical comparison of experimental EELS line scans with reconstructed ones from a model colloid, it has been possible to evidence a slight Sn surface enrichment equivalent to a submonolayer of pure Sn on the surface of the colloid.

Introduction

Pd−Sn Nanocolloids. Pd−Sn nanocolloids in acid suspension are widely used catalysts for the metallization of polymers.[1,2] A fundamental question is the structure and surface composition of the colloids. The relatively large enthalpy of mixing (down to −15 kcal/g atom at 320 K near the composition Pd_3Sn_2[3]) indicates the affinity of Pd and Sn; indeed, the Pd−Sn phase diagram[4] exhibits a large number of crystalline alloying phases: Pd_3Sn, Pd_2Sn, Pd_3Sn_2, PdSn, $PdSn_2$, $PdSn_3$, and $PdSn_4$. However, the surface energy of the two metals is very different: since tin has a surface tension about 3 times less than that of palladium,[5] one may expect a Sn segregation at the surface of Pd−Sn nanocolloids.

By Mössbauer spectroscopy experiments, Cohen and West[6−8] have established that Pd−Sn colloidal solutions, with an estimated size of the nanoparticles equal to 2 nm, contain metallic Pd and, to a lesser amount (i.e., ∼15 at. %), metallic Sn, both species being assumed to form a metallic core at the center of the nanocolloids. Further experimental evidence of stannous tin has been attributed to the existence of a shell consisting of $[SnCl_3]^-$ complexes, which act as surface stabilizing groups and avoid the agglomeration of colloids in the suspension.

High-resolution transmission electron microscopy (HRTEM) experiments of similar systems[9] showed that the core of such particles is crystalline and corresponds to the structure $PdSn_2$.

Despite these results, there is a lack of direct experimental evidence of the core−shell structure of Pd−Sn colloids, that is, of Sn surface enrichment. Therefore, the present TEM study has been undertaken to get local information about the core and surface composition of individual colloids.

TEM Studies of Bimetallic Layered Colloids. Bimetallic layered (core−shell) colloids have frequently been studied by TEM. Basically, the core−shell structure can be *directly* imaged under the following circumstances:

(i) If the core and the shell exhibit different atomic arrangements, then different lattice spacings can be resolved in HRTEM, which leads to a straightforward identification of the layered structure; such "polycrystalline" structures have, for example, been observed in Ag/Co particles with a typical size of 12 nm.[10]

(ii) If the atomic density of the core and the shell are sufficiently different, then phase and/or Fresnel contrast variations can occur radially from the center to the periphery of the

* To whom correspondence should be addressed. E-mail: thierry.epicier@insa-lyon.fr.
† GEMPPM.
‡ ATOFINA.

10.1021/jp026016o CCC: $25.00
Published on Web 02/04/2003

colloids: for example, the core can be imaged with a lighter contrast than the surrounding shell if it is filled with lighter elements and/or less atomic density than the shell. This method was used to characterize Ag/Au colloids in the size range of 10−16 nm by conventional TEM;[11] it appears that the core is filled with silver atoms (atomic number $Z_{Ag} = 47$) whereas the shell is made of gold ($Z_{Au} = 79$). Comparable results were produced in the case of CdS/HgS/CdS multilayered particles (with $Z_{Cd} = 48$ and $Z_{Hg} = 80$).[12]

(iii) Dedicated EFTEMs (energy-filtered transmission electron microscopes) may enable the core and shell regions to be imaged on the basis of their chemical differences: elemental maps can be produced by imaging the particles with electrons having experienced an energy loss corresponding to the excitation of a given element, provided the core and shell species are sufficiently different (i.e., have a large Z difference), their ionization edges are sharp enough to produce a good contrast, and the lateral size of each region is a noticeable fraction of a nanometer to fulfill the resolution restrictions of the technique.[14,15] Examples of such elemental maps have been produced for Ag−Co colloids, where the Ag core diameter and the Co shell thickness are about 8 and 2 nm, respectively.[10] A surface enrichment in calcium and iron has also been observed over several nanometers in aquatic iron-rich colloids (∼100 to 600 nm) by the same technique.[13]

Unfortunately, none of these conditions is met in the case of the much smaller Pd−Sn nanocolloids studied in the present work. First, no crystallographic difference is expected between the center and the periphery of the particles (since systematic alloying occurs because of the large enthalpy of mixing in the Pd−Sn system), although tin is expected to segregate but at an atomic level at the surface.[6−8] Second, no phase or Fresnel contrast variation can be expected (see point ii above) since Pd and Sn have very similar atomic weights ($Z_{Pd} = 46$ and $Z_{Sn} = 50$, which leads to a relative Z difference of $2(Z_{Sn} - Z_{Pd})/(Z_{Sn} + Z_{Pd}) \approx 8\%$, which is much lower than about 50% in the Ag−Au system[11] and in the Cd(S)−Hg(S) system,[12] where successful TEM work has been done). Finally, high-contrast elemental maps cannot be produced at a sufficient resolution by EFTEM for two main reasons: sharp-ionization Pd and Sn edges lie at very high energy losses (larger than 3 keV for the L2,3 edges) where the signal is too weak whereas edges at lower energy losses (M4,5 edges in the range of 330−600 eV) are not sharp enough to ensure good contrast (see the next section for more details on these edges). Moreover, the resolution required to image the expected Sn surface segregation (say, 0.1 or 0.2 nm) within nanometric Pd−Sn colloids cannot be achieved by this technique at the present time.

Thus, EELS analysis has been used in the present work according to a line-scan technique with a nanoprobe and a quantitative analysis of the EELS spectrum at each scan point, as explained in the next section.

Experimental Section

Sample Preparation. The industrial catalyst consists of Pd−Sn colloids suspended in a hydrochloric acid solution. They are charge stabilized with $[SnCl_3]^-$ groups[2]. The average size of the colloids has been measured using small-angle X-ray scattering (at the European Synchrotron Radiation Facility−ESRF, Grenoble, France):[16] an average radius of 2.52 nm with a relatively small size distribution has been measured.

A major disadvantage of the hydrochloric acid solution is that the colloid suspension could not be directly observed in HRTEM. Thus, dried samples were prepared by depositing a small droplet of the suspension onto a membrane of holey carbon supported by a Cu grid. To verify that the structure of the colloids was not significantly modified during this preparation process, quench-frozen solutions have been observed with a dedicated cryo-TEM. The comparison between the frozen preparations and the deposited dried colloids showed no difference in the size and shape of the colloids.[16] It is therefore assumed that the colloids are not altered by the drying procedure.

TEM and EELS Work. HRTEM observations were done on an FEG-TEM instrument working at 200 kV (JEOL 2010F[17]). Probes in the range of 0.4 to 1 nm were used to acquire a series of EELS spectra across individual particles (line-scan or line-spectrum technique); the probe was monitored either manually (calibrated beam shifts with the microscope controls) or with an OXFORD semi-STEM (scanning TEM) device. EDX (energy-dispersive X-ray) spectroscopy was performed with an OXFORD Link-Isis analyzer to get the average composition of individual colloids.

EELS spectra were obtained on the FEG-TEM microscope with a GATAN Parallel EELS spectrometer in the nanoprobe mode. The usual corrections were performed on these experimental spectra before analysis (see ref 18 and below for the background subtraction), except the thickness deconvolution, since a low-loss spectrum is not available at each point of the scan. However, mean low-loss spectra recorded on many colloids show that the effect of the thickness is negligible as intuitively expected, since only regions with a thickness on the order of nanometers were investigated. For the same reason, the beam spreading within the thin colloid was neglected.

Spectra were acquired with counting times on the order of 2 s in an energy-loss range of 250−750 eV including the Pd-M4,5 (starting at 330 eV) and the Sn-M4,5 edges (starting at 485 eV). These edges present the advantage of lying in a relatively low energy-loss range (compared to those of the Pd-L2,3 and Sn-L2,3 at about 3.3 and 4.0 keV, respectively, and too far for a nanoprobe analysis) and on the same side with respect to the carbon K edge near 284 eV. One problem is, however, that these M edges are not far above the C K edge: they are therefore strongly influenced in the case of particles supported on a carbon film. The study was then restricted to colloids strictly located at the border of the carbon film in order to minimize the influence of the C K edge. For the spectra where the carbon K edge was detected, a spectrum recorded on the carbon film was used as a background model and subtracted from the original spectra.[19] Since (Sn, Cl) complexes are expected to stabilize the colloids (see above), it would have been interesting to quantify a Cl edge (i.e., the L edge starting near 200 eV). The undesirable influence of the C K edge has unfortunately led us to disregard the Cl L edge because this peak is lying at the opposite side of the C K edge, which makes the background subtraction very difficult from about 200 to 600 eV in the presence of carbon.

Another problem is that the maximum of the oxygen K edge at 536 eV nearly coincides with that of the Sn M edge, which may affect the analysis if the colloids are partially oxidized. However, the Sn M-edge maximum is very broad whereas the O K edge has significant fine structure, which makes it easy to detect oxygen (see the comparison between the pure Sn spectrum and the SnO_2 spectrum in Figure 1); great care has been taken regarding this point, and it was found that most colloids were oxygen-free.

Quantitative Analysis of EELS Line Scans. The line scans have been evaluated by comparing the experimental spectra to

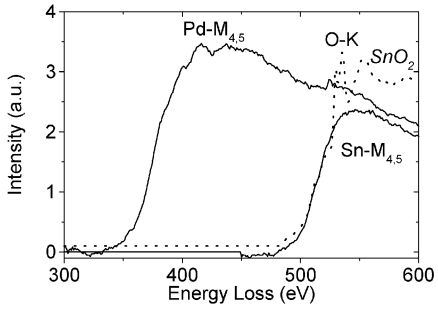

Figure 1. Normalized reference EELS spectra for the Pd-M4,5 and Sn-M4,5 edges in pure Pd, pure Sn, and SnO_2 (- -) particles.

reconstructed spectra obtained from a computer experiment on a model colloid; the full procedure has been detailed elsewhere[19] and can be summarized as follows. A core−shell colloid is geometrically modeled and filled randomly with atoms (e.g., Pd and Sn atoms) according to the density of pure elements (respectively, 68 and 29.1 atoms/nm^3) and the Sn/Pd atomic ratio deduced from the experiment (see below). In the computer experiment, a virtual scan is performed on a model colloid. At each position of the computed line scan, the number of atoms in the electron beam is counted, and then EELS spectra can be reconstructed by weighting normalized reference spectra of Pd and Sn (see Figure 1) with the number of atoms. The crucial parameters of the calculation are (i) the scan parameters (i.e., the electron-beam probe size expressed as the full width at half maximum (fwhm)), the step width between individual spectra (these parameters being known from previous calibrations), and the start position of the probe and (ii) the colloid geometry and chemistry (i.e., the core and shell radii and the respective concentrations of Sn and Pd species in the core and shell regions). Some of these parameters were deduced from the experiment: the total size of the particle could be estimated from HRTEM micrographs, and the mean composition (fixing the core concentrations) of the particle was measured from EDX analysis. The shell was in fact considered to be a pure Sn layer, which can be used to describe any Sn surface enrichment.

The unfixed parameters of the calculation were allowed to vary systematically within realistic ranges. For each set of geometrical and chemical configurations of the model, the atomic arrangement of the colloid was generated several times and averaged to get a better statistical description of the colloids.[19] Finally, the computer analysis leads to several hundred models, the reconstructed spectra of which are then compared to the experimental spectra and sorted by order of merit with a least-squares fitting procedure: the best matching model could then be found at the minimum of the quality factor.

Results and Discussion

Figure 2 is a low-magnification TEM micrograph showing the distribution of the colloids when deposited on a holey carbon-coated Cu grid.

The particle size is in good agreement with the average size mentioned above (i.e., 2.52 nm), although colloids in the range of 4 to 5 nm can be observed.

Figure 3 shows a typical HRTEM micrograph of Pd−Sn nanocolloids located at the border of a hole on the carbon film; by chance, one of those particles exhibits a sharp lattice contrast, which enables its crystallographic indexing by its diffractogram (Fourier transform of the image). The Pd_3Sn_2 hexagonal phase (S. G.: $P6_3/mmc$; $a = 0.4390$ nm, $c = 0.5655$ nm) is unambiguously identified.

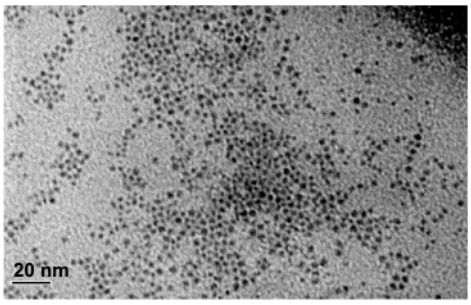

Figure 2. Pd/Sn nanocolloids as observed in conventional TEM.

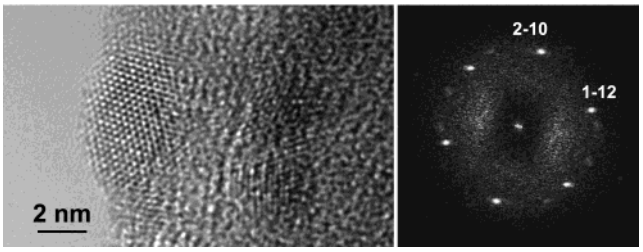

Figure 3. Pd/Sn particle situated at the border of a hole on the carbon film. The associated diffractogram shows the [241] azimuth of Pd_3Sn_2.

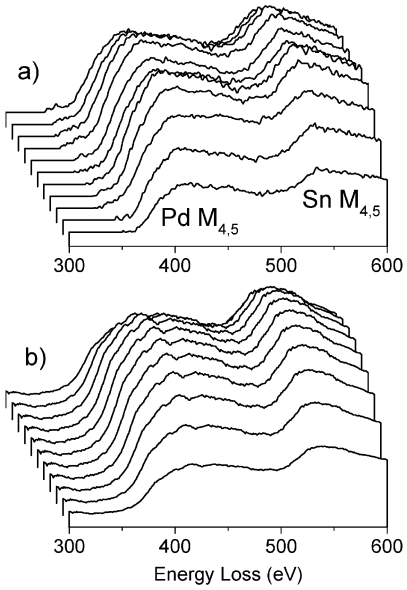

Figure 4. (a) Experimental line scan across the colloid shown in Figure 3, with a step width of 0.35 nm between each spectrum and (b) reconstructed line scan from the best matching model (see particle 1 in Table 1). In both montages, the top spectrum has been acquired on the vacuum side, and the bottom spectrum, on the carbon film side.

An EELS line scan, with a step width between each spectrum of 0.35 nm and a probe size (fwhm) of 0.7 nm, has been performed on this colloid (Figure 4 a). Note that the size of this particle is about 4.5 ± 0.5 nm.

The result of the evaluation of the line scan with the method described above is illustrated in Figures 4 b and 5. In the top diagram of Figure 5a, the quality factor is plotted versus the shell thickness, all other parameters of the model being optimized at each point. This diagram clearly shows that the core−shell model is better than the homogeneous model (i.e., a colloid with no shell (shell thickness = 0)). In the bottom diagram of Figure 5a, a similar plot is shown as a function of the Sn core concentration; the optimum is found at 39%, which agrees very well with the composition deduced from the

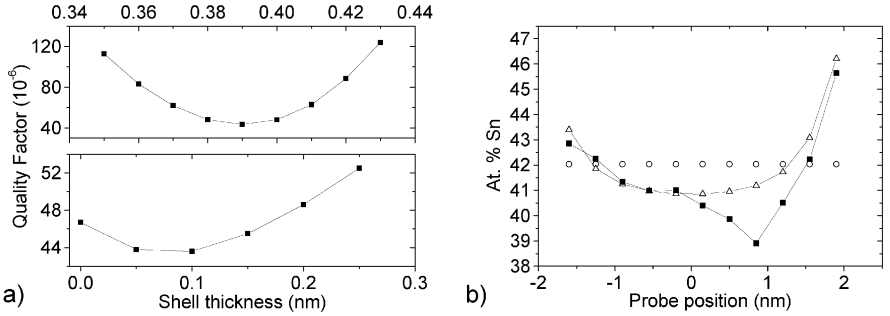

Figure 5. Results of the treatment: (a) quality factors when changing the shell thickness (top) and the Sn core concentration (bottom); (b) experimental Sn/Pd ratio (■) compared to that of the model colloid with (△) and without (○) Sn surface enrichment.

TABLE 1: Evaluation of Line Scans Performed on Different Colloids

particle number	average composition[a]	Sn core concentration (at. %)	equivalent 100% Sn shell thickness (nm)
1	Pd_3Sn_2	39	0.10
2	$\sim Pd_2Sn$	31	0.15
3	$\sim Pd_2Sn$	30	0.15
4	Pd_2Sn	33	0.10

[a] EDX measurement.

crystallographic analysis (i.e., Pd_3Sn_2, corresponding to [Sn] = 40 at. %).

Three other colloids nicely located at the border of the carbon film have been analyzed by the same procedure. Those particles were generally imaged by a monodimensional set of lattice fringes but were not conveniently oriented with respect to the electron beam; thus, the crystallographic indexing, such as that presented in Figure 3, could not have been performed. (It should be mentioned here that most of the (Pd, Sn) structures have close-packed distances very close to that of the fcc Pd phase, which makes their crystallographic indexing almost impossible under these conditions.) The results are summarized in Table 1.

A slight Sn enrichment, corresponding to a Sn submonolayer, has been observed for all experiments. This corresponds roughly to a replacement of Pd atoms by Sn on low coordination sites at the surface, which are, from a thermodynamic point of view, the first atoms that have to be replaced (see, for example, refs 20 and 21). Since the heat of mixing of Pd and Sn is relatively large,[3] it is not reasonable to expect a more pronounced surface segregation than the one observed.

Figure 5b shows the complete results, in terms of the Sn/Pd atomic ratio, for the line scan analyzed in Figure 4. This diagram again illustrates the fact that the core−shell model is in better agreement with the experiment than is the homogeneous model. However, experimental data deviate from the deduced core−shell model for the first and last six probe positions: the first and last points have been acquired on the edges of the particle, where the signal-to-noise ratio is very weak. In the second half of the line-scan (i.e., the six later points), the Sn enrichment seems to be different than that predicted by the best core−shell model; for those positions, original spectra show an increasing C K edge, which indicates that the probe touches the carbon supporting film. The possible explanation is that the carbon film itself may have absorbed Sn ions or that the colloid is "glued" to the carbon support by Sn complexes. A similar result has been obtained for supported Pt/Sn-catalysts, the Pt particles being anchored to their support by Sn[22] or Sn−O bridges.[23]

The HRTEM and EELS analyses of individual Pd−Sn colloids show that their core consists of a crystallized (Pd, Sn) alloy with different Sn concentrations present. Furthermore, the EELS line-spectrum technique in a nanoprobe mode has evidenced a slight enrichment of Sn at the external surface of the colloids, corresponding to less than a pure Sn monolayer. Although the experimental results are near the limits of performance of the TEM technique, this result has been obtained on several particles, which gives the first direct evidence of the core−shell structure of such Pd−Sn colloids.

Acknowledgment. One of the referees is gratefully acknowledged for having informed us about some pertinent works published in the literature.

References and Notes

(1) Ono, S.; Osaka, T.; Naitoh, K.; Nakagishi, Y. *J. Electrochem. Soc.* **1999**, *146*, 160.
(2) Middeke, H. *Galvano-Organo-Trait. Surf.* **1998**, *685*, 357.
(3) Hultgren, R. et al. *Selected Values of the Thermodynamic Properties of Binary Alloys*; American Society for Metals: Metals Park, OH, 1973; Vol. 2.
(4) Massalski, A. T. B.; Murray, J. L.; Bennett, L. H.; Baker, H. *Binary Alloy Phase Diagrams*; American Society for Metals: Metals Park, OH, 1986; Vol. 2.
(5) Yaws, C. L. *Chemical Properties Handbook: Physical, Thermodynamic, Environmental, Transport, Safety, and Health Related Properties for Organic and Inorganic Chemicals*; McGraw-Hill: New York, 1999.
(6) Cohen, R. L.; West, K. W. *Chem. Phys. Lett.* **1972**, *13*, 482.
(7) Cohen, R. L.; West, K. W. *Chem. Phys. Lett.* **1972**, *16*, 128.
(8) Cohen, R. L.; West, K. W. *J. Electrochem. Soc.* **1973**, *120*, 502.
(9) Froment, M.; Queau, E.; Martin, J. R.; Stremsdoerfer, G. *J. Electrochem. Soc.* **1995**, *142*, 3373.
(10) Sobal, N.; Hilgendorff, M.; Möhwald, H.; Gersig, M.; Spasova, M.; Radetic, T.; Farle, M. *Nano Lett.* **2002**, *2*, 621.
(11) Srnova-Sloufova, I.; Lednicky, F.; Gemperle, A.; Gemperlova, J. *Langmuir* **2000**, *16*, 9928.
(12) Mews, A.; Eychmüller, A.; Giersig, M.; Schooss, D.; Weller, H. *J. Phys. Chem.* **1994**, *98*, 934.
(13) Mondi, C.; Leifer, K.; Macrovodatos, D.; Perret, D. *J. Microsc. (Oxford)*, submitted for publication, 2002.
(14) Krivanek, O. L.; Kundmann, M. K.; Kimoto, K. *J. Microsc. (Oxford)* **1995**, *190*, 277.
(15) Egerton, R. F.; Crozier, P. A. *Micron* **1997**, *28*, 2.
(16) Holderer, O.; David, L. P.; Delichere, P.; Epicier, T.; Esnouf, C.; Fuchs, G. *J. Phys. IV* **2002**, *12*, Pr6−499.
(17) *CLYME: Consortium LYonnais de Microscopie Electronique*: INSA: Villeurbanne, France.
(18) Egerton, R. F. *Electron Energy-Loss Spectroscopy in the Electron Microscope*, 2nd ed.; Plenum Press: New York, 1996.
(19) Holderer, O.; Sennour, M.; Epicier, T.; Esnouf, C. *Ultramicroscopy*, submitted for publication, 2002.
(20) Rousset, J. L.; Renouprez, A. J.; Cadrot, A. M. *Phys. Rev. B* **1998**, *58*, 2150.
(21) Strohl, J. K.; King, T. S. *J. Catal.* **1989**, *119*, 540.
(22) Meitzner, G.; Via, G. H.; Lytle, F. W.; Fung, S. C.; Sinfelt, J. H. *J. Phys. Chem.* **1988**, *92*, 2925.
(23) Caballero, A.; Dexpert, H.; Didillon, B.; LePeltier, F.; Clause, O.; Lynch, J. *J. Phys. Chem.* **1993**, *97*, 11283.